1. Physiography of the Laguna Azul-Lago Sarmiento Area

The Torres del Paine region is in the only continental landmass at these southern latitudes (51ºS) and is in the subantarctic climatic zone affected by the south westerly wind belt. This wind system transports cyclones northward that originate in the Antarctic Frontal Zone (AFZ) and is associated with elevated precipitation (Garreaud, 2007). For comparison, during the Last Glacial Maximum (LGM) the westerly belt is thought to have shifted as far north as ~40ºS (Moreno et al., 1999; Lamy et al., 2004), affecting climate and glacier dynamics all along the southern Andes in response to its direct influence on the Patagonian ice sheet mass balance. The present ice fields in Patagonia (Northern and Southern Patagonian Ice Fields) extend 17,200 km^2 (Aniya et al., 1996; Aniya and Wakao, 1997) along the southern Andes. The Torres del Paine field area occurs in the lee of the Andes adjacent to the southeastern tip of the Southern Patagonian Ice Field. The present-day equilibrium line altitude (ELA) throughout this ice field varies from about 900-1400 m a.s.l. (Cassasa et al., 2002), which demonstrates the significant geographical (especially west to east; Warren and Sudgen, 1993) variability among outlets draining the ice field.

During late-glacial time, outlet glaciers draining the Patagonian ice sheet and the alpine Cordillera Paine ice cap in Torres del Paine coalesced to form three main but connected lobes: Laguna Azul, Lago Sarmiento and Lago del Toro ice lobes. At this time, low-surface gradient glacier ice extended about 45 km beyond the present ice terminus at the Southern Patagonian Ice Field and shaped the Torres del Paine landscape (Fig. DR1).

The overall landscape in Torres del Paine shows classical, glacially scoured morphology, interrupted by deep, elongated, west-east troughs occupied by lakes (Fig. DR1). These lakes are settled within a dramatic, high-relief topography and fringed at their eastern margins by thick glacial deposits, including the distinctive four TDP moraine belts (TDP I, II, III and IV) and associated outwash plains. The TDP II, III and IV moraines are morphologically distinct and mostly continuous between lake basins. Each of the TDP II and TDP III moraines comprise 5-10 sharp, well-defined ridges (main manuscript Fig. 2; Fig. DR2). TDP IV moraines are less prominent and commonly occur as two parallel well-defined moraine ridges. The oldest TDP I moraine is a wider, smoothed, much more prominent landform when compared with the TDP II, III and IV moraines (Marden and Clapperton, 1995; Marden, 1997).

Laguna Azul (220 m a.s.l.) and Lago Sarmiento (75 m a.s.l.) occupy the bottom of two independent basins, separated by ~12 km of open, low-relief, bedrock-controlled topography (~500-250 m a.s.l., Fig. DR1). The surface here is mantled with a relatively thin glacial drift, sprinkled with small dry lake bodies and crossed by north-south moraine ridges. The outer moraines, marked in part by boulder lines, are mostly uninterrupted between Laguna Azul and Lago Sarmiento, and define an exceptionally sharp glacial-drift limit (Fig. DR2). Between these two lakes, south of Laguna Azul,

glacier ice was buttressed against eastern foothills, where it cut west-east channel conduits that carried meltwaters from the ice front. A prominent example is the Cañadon del Macho meltwater channel that interrupts the continuity of TDP II, III and IV moraines. At least two terrace levels are present in this channel and proximal glaciofluvial sediments are as much as boulder size. Vega Capón/Baguales is another meltwater channel occurring to the north of the study area (Fig. 2, main manuscript) that during the TDP II, III and IV advances carried meltwater into the paleo Río de las Chinas.

2. Radiocarbon Ages

In this study we dated a gastropod shell layer (laboratory sample OS-74487; Sample ID LC_03) close to the base of a core extruded at Vega Baguales (Figure DR1; Fig. 2, main manuscript). All radiocarbon ages in this work were calibrated using the IntCal09 curve by Reimer et al. (2009). In the text, we use the mean and standard deviation of the population with the greatest probability (bolded values) for discussion.

- Vega Baguales. Sample LC_03 ($\delta^{13}C$ -4.12‰): 10,550 ± 55 ^{14}C years B.P.
  Calibrated age (1σ range):
  12,424 - 12,492 cal B.P. (0.53448)
  12,516 - 12,572 cal B.P. (0.46552)
  Mean: 12,460 ± 70 cal yrs B.P. (0.53448)

Calibration of radiocarbon ages published by Moreno et al. (2009) include:

- Vega Ñandu. Sample PS0304A T4_398-400: 10,555 ± 40 ^{14}C years B.P.
  Calibrated age (1σ range):
  12428 - 12476 cal B.P. (0.458398)
  12521 - 12575 cal B.P. (0.541602)
  Mean: 12,550 ± 40 cal yrs B.P. (0.541602)

- Lago Calvario. Weighted mean: 10,492 ± 45 ^{4}C years B.P.
  Calibrated age (1σ range):
  12406 – 12542 cal B.P. (1)
  Mean: 12,475 ± 95 cal yrs B.P.

- Vega Capón. Weighted mean: 10,418 ± 49 ^{14}C years B.P.
  Calibrated age (1σ range):
  12,149 – 12,191 cal B.P. (0.166451)
  12,211 – 12357 cal B.P. (0.634385)
  12368 - 12413 cal B.P. (0.199163)
  Mean: 12,285 ± 105 cal yrs B.P. (0.634385)

- Puerto Bandera moraines (Strelin et al., 2011). Mean: 11,100 ± 60 ^{14}C years B.P.
  Calibrated age (1σ range):
  12,914 - 13,100 cal B.P. (1)

Mean: 13,000 ± 130 cal yrs B.P.

3. ^{10}Be Surface Exposure Dating

3.1 Sampling Protocol and Assumptions

We sampled boulders with quartz-bearing lithologies (mostly granite, greywacke and dacite) embedded in or resting on stable moraine crests (Fig. DR2). Sampled boulder surfaces (usually upper 2 cm) were mostly horizontal (≤10º) and very well preserved. We avoided weathered surfaces and boulders with clear erosional signs, such as deep cracks and fractured tops, rainwater corrosion or exfoliation (Putnam et al., 2010a). Minimum height of boulders was ~65 cm and most were between 100 and 200 cm. Some samples were from striated boulder surfaces, which afforded evidence for minimal erosion.

There is limited information on the spatial and temporal variability in erosion rates in Patagonia (Kaplan et al, 2005; Douglass, 2005). At Lago Buenos Aires, preliminary maximum estimates based on a limited number of samples varied between 1.0 to 2.3 mm per 1000 years, with an average of 1.4 mm per 1000 years during long exposure times (10^5 years). In addition, Douglass (2005) at the same site, with additional data, reported erosion rates of <1 mm per 1000 years. A value of 1.4 mm/kyr should be taken as provisional because it comes from only a few boulders at a single site in central Patagonia and is only maximum rates. If we apply an erosion rate of 1.4 mm per 1000 years to Laguna Azul and Lago Sarmiento samples, TDP exposure ages would increase by ~1.5%, which does not affect our conclusions. Given that we preferentially sampled well-preserved boulder tops, we assume no erosion effect in our age calculations. The fact the sample exposure time corresponds to the last ~14 ka years, mostly under a warm and dry interglacial climate (Lamy et al., 2010), may have favored local landscape stability.

Snow shielding may affect the production rate of cosmogenic nuclides when the seasonal snowpack is thick (e.g. greater than one meter) and lingers for a number of months on top of rock surfaces (Jackson et al., 1999). Average winter temperature in Torres del Paine is >0ºC (Carrasco et al., 2002) close to where the moraine belts are located, which makes thick snow accumulation for long periods unlikely. The Southern Andes relief enhances regional orographic precipitation and produces a sharp precipitation gradient between west and east across the Andes, with the eastern sides receiving only 5% of the precipitation recorded at the western coast (Carrasco et al., 2002). Rock samples for cosmogenic-exposure dating were obtained from areas below 400 m a.s.l., distant from the mountain front (~45 km from present ice margins), near the steppe-forest ecotone border, and in locations exposed to the wind which would inhibit snow accumulation on rock surfaces. Therefore, we assume snow build up on moraine crests and boulder tops is minimized.

The semiarid condition in the Torres del Paine region produces the well-known steppe plains of eastern Patagonia, with the last forest remains present at the foothills of the Andes. Although pollen records show forest being more generally distributed in

Torres del Paine during the mid-Holocene (Moreno et al., 2010), the eastern area of the park has remained at the forest-steppe ecotone. There is no soil or pollen evidence for thick forests that would have shielded our boulders and thus affected ^{10}Be cosmogenic nuclide history.

3.2 Sample Preparation and Analysis

Sample preparation and beryllium extraction was carried out in the laboratory facilities of the Earth Sciences Department and Climate Change Institute at the University of Maine (UMAINE), and in the Cosmogenic Nuclide Laboratory at Lamont Doherty Earth Observatory (LDEO). We followed standard laboratory protocols explained in Schaefer et al. (2009) and at http://LDEO_Cosmogenic_Nuclide_Lab/Chemistry. In the UMAINE facilities we separated and obtained clean quartz samples. The final procedural steps including dissolution of quartz, ^{10}Be extraction, and cathode loading were carried out at LDEO. We use a low background ^{9}Be carrier that leads to a low-ratio process blank (blank ^{10}Be/^{9}Be range is from $3.240 \times 10^{-16} \pm 1.237 \times 10^{-16}$ to $1.416 \times 10^{-15} \pm 4.130 \times 10^{-16}$). The number of ^{10}Be atoms in these process blanks ranged from 4.350×10^{3} to 1.7060×10^{4}. For comparison, the samples contained ~2×10^{5} to 2×10^{6} ^{10}Be atoms. Blank correction ranged from 0.3 to 10.8%. All this led to age results well above process blanks with ^{10}Be/^{9}Be ratios as low as 10^{-14}-10^{-15} and significant improvement in the precision of our ages compared to prior studies in the area (see technical details in Schaefer et al., 2009).

Accelerator mass spectrometer (AMS) ^{10}Be/^{9}Be analysis was carried out at the Lawrence Livermore National Laboratory (LLNL), which resulted in ^{10}Be/^{9}Be ratios with low analytical errors that range between 2.0% and 8.4% and average 3.9% (Fig. DR3). All samples and blanks were measured relative to the 07KNSTD standard, with a $(2.79 \pm 0.03) \times 10^{-11}$ ^{10}Be/^{9}Be and ^{10}Be half-life of $(1.36 \pm 0.07) \times 10^{6}$ yr (Nishiizumi et al., 2007). Table DR1 shows the analytical data from our samples in Torres del Paine.

3.3 ^{10}Be Production Rate (PR)

To calculate the exposure ages of our samples, we used the ^{10}Be PR derived at New Zealand's Macaulay site (43ºS; Putnam et al., 2010b), which is based on a 9,690 ± 50 cal year B.P. landslide. The PR value derived at the Macaulay site, the only previously available for the mid latitudes of the southern hemisphere, was recently confirmed at two sites <100 km to the north in the Lago Argentino basin (Kaplan et al., 2011) from similar elevations as our samples (and for the same time period as discussed here). For comparison, we also present in Table DR2 ^{10}Be ages from the commonly used "CRONUS calibration data set" PR (Balco et al., 2008); the average difference between the ^{10}Be ages is 14.2%, with the ages being ~1,000-3000 years younger when using the "CRONUS calibration data set".

In addition, radiocarbon dating at the Vega Baguales meltwater channel in Torres del Paine (50º53'47''S; 72º44'35''W, 455 m a.s.l. Fig. DR1 and DR4; Fig. 2, main manuscript), which served as a main conduit for meltwater escaping the ice front when it

was at TDP II, III and IV moraines, represents an opportunity to test the local validity of both PRs used in our study. A piston core extruded from the distal part of the channel exhibits at the base glaciolacustrine rhythmites made up of fine sand and muddy layers, overlain first by coarser sand containing very well preserved gastropods shells and subsequently by organic silt and fiber-rich sediment. A ^{14}C age of 10.6 ± 0.05 (1σ) ^{14}C kyr B.P. (calibrated age of 12.5 ± 0.07 (1σ) kcal yr B.P.; IntCal09 curve, Reimer et al., 2009) obtained from a gastropod shell close to the base of the core (272 cm depth) defines a minimum age for abandonment of this conduit after ice retreat from TDP IV position. This minimum deglacial age is statistically indistinguishable (i.e., overlaps at 1σ) from that obtained in previous work (Moreno et al., 2009) from Vega Capón, a site located less than one kilometer in the up-ice direction along the same channel. The date is also similar to those from other sites in Torres del Paine (Moreno et al., 2009; main manuscript Fig. 2; Fig. DR1). These radiocarbon ages suggest that by 12.5 ka there was no ice occupying the proximal part of Vega Capón and therefore ice had retreated from the late-glacial moraines. Moreover, evidence from the distal core in Vega Baguales shows that the meltwater conduit was abandoned by this time and organic remains had begun to accumulate. This scenario and the radiocarbon ages for ice recession are in conflict with most of the ^{10}Be ages produced by the "CRONUS calibration data set" (Balco et al., 2008). On the other hand, the New Zealand's PR (Putnam et al., 2010b), recently confirmed in the nearby Lago Argentino area (Kaplan et al., 2011), yields consistent ^{14}C and ^{10}Be chronologies.

3.4 Outlier Detection and Rejection

In order to detect and reject outliers, we applied the Grubbs test (Grubbs, 1969) to the age population of each of the three moraines in Torres del Paine: TDP II, TDP III and TDP IV. We also treated sample ages that were more than 2σ from the arithmetic mean moraine age as outliers. However, choosing 2σ or 3σ does not affect our conclusions. Figure DR5 illustrates moraines age distributions shown as probability plots after outlier rejection. For TDP IV we included and recalculated two CAMS ^{10}Be ages (Moreno et al., 2009) using the New Zealand production rate (Putnam et al., 2010b). The Grubbs test detected (with 99% confidence level) three outliers in TDP II moraine age population: samples LA0714, LA0716 and LA0732. In the same moraine belt, these samples plus SAR0719 and SAR0702 are >2σ from the arithmetic mean and are also considered outliers. LA0512, LA0701, LA0724 and LA0906 ages from TDP III moraine are >3σ different from the mean age of the TDP III moraine, and therefore we consider them as outliers. SAR0722 in TDP IV is >2σ from the arithmetic mean moraine age and therefore was also treated as an outlier.

Outlier ages may be due mainly to post-depositional geomorphic processes. A discrete group of outliers includes anomalously young ages (samples LA0512, LA0714, SAR0701, SAR0906) that date to the Early Holocene. Because erosion rates seem to be low at the study area (see above; Kaplan et al, 2005; Douglass 2005), this group of outliers most likely indicates post-depositional landform adjustments. However, 8% of the ^{10}Be ages date to the LGM and beginning of the Termination (Samples LA0716, LA0732, SAR0722, SAR0724), and thus form a group of outliers older than the sample

mean. These boulders may reflect reworked samples; the ice margin may have incorporated boulders from older glacial deposits into younger moraines. Most of the detected outliers are significantly different from the mean age of the respective moraine. Only two samples identified as outliers were only slightly more than 2σ from the mean (samples SAR0719 and SAR0702).

After rejecting outliers from the data set we obtained tighter clusters of dates for each TDP moraine (Fig. DR5). Overall, the individual analytical errors are comparable with the standard deviation of the mean age of each moraine (~4%), particularly TDP II and III, suggesting that in most cases the scatter in the mean age of the moraines can be explained by analytical uncertainties. Also, the chi-squared (χ_2) for each TDP moraine data set is ≤1, indicating normal distribution after outlier rejection.

3.5 ^{10}Be Ages Calculation

After rejecting outliers we calculated the arithmetic mean for each TDP moraine data set: TDP II, III, IV. Associated errors include the propagation of internal (i.e., analytical) and external (e.g., production rate) uncertainties (see Fig. DR5). As suggested by Putnam et al. (2010b), we used the 2.4% uncertainty of the New Zealand production rate. Scaling to the Torres del Paine region is assumed free of uncertainty (cf., Kaplan et al., 2011).

The uncertainties for the arithmetic mean of each TDP moraine systems were then calculated in quadrature as follows:

TOTAL UNCERTAINTY (1 σ): SQRT (((STDEV^2)+(MEAN*0.024)^2))) .

4. The Southern Glaciers During ACR (Fig. 4)

Glaciers in Patagonia are particularly sensitive to climate change (Oerlemans, 2005; Rignot et al., 2003; Keer and Sugden, 1994). Prominent late glacial readvances coincident with the Antarctic Cold Reversal (ACR) interrupted the last deglaciation in the south mid latitudes. Figure 4 (main manuscript) shows times at which late glacial expansions peaked in both south Patagonia and the Southern Alps of New Zealand. Glacier records from the Tasman River-Lake Pukaki (Putnam et al., 2010a) and Irishman Stream basins (Kaplan et al., 2010) in New Zealand afford evidence for glacier culmination close to 13,000 ± 500 a, which is supported on the western side of the Southern Alps by the contemporaneous late glacial advance of the Franz Josef Glacier (Denton and Hendy, 1994; Turney et al., 2007). On the east side of the Pacific Ocean, in Patagonia, late glacial expansion at about 13,000 years ago is also found at Lago Argentino (Strelin et al., 2011). Here, Strelin et al., revealed that the Lago Argentino glacier (50ºS) expanded and deposited the Puerto Bandera moraines at or slightly after 12,990 ± 80 cal yrs B.P. Interestingly, the late glacial record from Torres del Paine (51ºS) suggests that the ice expanded by 14,200 ± 560, significantly earlier than these studies. Nonetheless, on the South Island of New Zealand, two boulders on a moraine outboard of the Birch Hill I ridge (13,000 ± 300 a, Lake Pukaki) gave a mean age of

14,100 ± 300 a (Putnam et al., 2010a) comparable within uncertainties with our results and with previous broad dating (Moreno et al., 2009) of the TDP IV moraines in Torres del Paine (Fig. 4). Thus, the late glacial record from Torres del Paine and potentially in New Zealand indicate an early ACR glacial phase in the southern mid latitudes and that southern glaciers expanded not only at the end of the ACR but throughout this period (Fig. 4, main manuscript).

5. References Cited

Aniya, M., Sato, H., Naruse, R., Skvarca, P., Cassasa, G., 1996, Remote sensing application to inventorying glaciers in a large, remote area-Southern Patagonia Icefield: Photogrammetric Engineering and Remote Sensing, v. 62, p. 1361-1369.

Aniya, M. and Wakao, Y., 1997, Glacier variations of Hielo Patagónico Norte, Chile, between 1944/45 and 1995/95: Bulletin of Glacier Research, v. 15, p. 11-18.

Balco, G., Stone J., Lifton N., Dunai T., 2008, A complete and easily accessible means of calculating surface exposure ages or erosion rates from 10Be and 26Al measurements: Quaternary Geochronology, v. 3, p. 174-195.

Carrasco, J. F., Cassasa, G., Rivera, A., Aniya, M., Naruse, R., 2002, Meteorological and climatological aspects of the Southern Patagonia Icefield., *in* Cassasa, G., Sepúlveda, F.V., Sinclair, R.F. eds., The Patagonian Icefields, New York, Kluwer Academic/Plenum Publishers, p. 29-41.

Cassasa, G., Rivera, A., Aniya, M., Naruse, R., 2002, Current knowledge of the southern Patagonia Icefield, *in* Cassasa, G., Sepúlveda, F.V., Sinclair, R.F. eds., The Patagonian Icefields, New York, Kluwer Academic/Plenum Publishers, p 67-83.

Denton, G.H. and Hendy, C.H., 1994, Younger Dryas age advance of Franz Josef Glacier in the Southern Alps of New Zealand: Science, v. 264, p. 1434-1437.

Desilets, D. and Zreda, M., 2003, Spatial and temporal distribution of secondary cosmic-ray nucleon intensities and applications to in-situ cosmogenic dating: Earth and Planet. Sci. Lett., v. 206, p. 21- 42.

Douglass, D.C., 2005, Glacial chronology, soil development, and paleoclimate reconstructions for mid-latitude South America, 1 Ma to recent [Ph.D. thesis]: Wisconsin, University of Wisconsin.

Dunai, T.J., 2001, Influence of secular variation of the magnetic field on production rates of in situ produced cosmogenic nuclides: Earth and Planet. Sci. Lett., v. 193, p. 197-212.

Garreaud, R.D., 2007, Precipitation and Circulation Covariability in the Extratropics: Journal of Climate, v. 20, p. 4789-4797.

Grubbs, F.E., 1969, Procedures for detecting outlying observations in samples: Technometrics, v. 11, p. 1-21.

Jackson, L.E., Phillips, F.M., Little, E.C., 1999, Cosmogenic 36Cl dating of the maximum limit of the Laurentide Ice Sheet in southwestern Alberta: Canadian Journal of Earth Sciences, v. 36, p. 1347–1356.

Kaplan, M. R., Douglass, D. C., Singer, B. S., Ackert, R. P., Caffee. M.W., 2005, Cosmogenic nuclide chronology of pre-last glacial maximum moraines at Lago Buenos Aires, 46ºS, Argentina: Quaternary Research, v. 63, p. 301–315.

Kaplan, M.R., Schaefer, J.M., Denton, G.H., Barrell, D.J.A., Chinn, T.J.H., Putnam, A.E., Andersen, B.G., Finkel, R.C., Schwartz, R., and Doughty, A.M., 2010, Glacier retreat in New Zealand during the Younger Dryas stadial: Nature, v. 467, p. 194-197.

Kaplan, M.R., Strelin, J.A., Schaefer, J.M., Denton, G.H., Finkel, R.C., Schwartz, R., Putnam, A.E., Vandergoes, M.J., Goehring, B.M., Travis, S.G., 2011, In-situ cosmogenic ^{10}Be production rate at Lago Argentino, Patagonia: Implications for late-glacial climate chronology: Earth and Planetary Science Letters, v. 309, p. 21-32.

Keer, A., and Sugden, D.E., 1994, The sensitivity of the South Chilean snowline to climatic change: Climatic Change v. 28, p. 255-272.

Lamy, F., Kaiser, J., Ninnemann, U., Hebbeln, D., Arz, H.W., and Stoner, J., 2004, Antarctic Timing of Surface Water Changes off Chile and Patagonian Ice Sheet Response: Science, v. 304, p. 1959-1962.

Lamy, F., Kilian, R., Arz, H.W., Francois, J.P., Kaiser, J., Prange, M. Steinke, T., 2010, Holocene changes in the position and intensity of the southern westerly wind belt: Nature Geoscience, v. 3, p. 695-699.

Lifton, N., Smart, D., Shea, M., 2008, Scaling time-integrated in situ cosmogenic nuclide production rates using a continuous geomagnetic model: Earth and Planet. Sci. Lett., v. 268, p. 190-201.

Marden C. J. and Clapperton, C. M., 1995, Fluctuations of the South Patagonia Icefield during the last glaciation and the Holocene: Journal of Quaternary Science, v. 10, 197-210.

Marden, C. J., 1997, Late-glacial fluctuations of South Patagonian Icefield, Torres del Paine National Park, southern Chile: Quaternary International, v. 38-39, p. 61–68.

Moreno, P.I., Jacobson G.L., Andersen B.G., Lowell T.V., Denton G.H., 1999, Abrupt vegetation and climate changes during the last glacial maximum and last termination in the Chilean Lake District: A case study from Canal de la Puntilla (41ºS): Geografiska Annaler, v. 81A, p. 285-311.

Moreno, P.I., Kaplan, M.R., Francois, J.P., Villa-Martinez, R., Moy, C.M., Stern, C.R., and Kubik, P.W., 2009, Renewed glacial activity during the Antarctic cold reversal and persistence of cold conditions until 11.5 ka in southwestern Patagonia: Geology, v. 37, p. 375-378.

Moreno, P.I., Francois, J.P., Villa-Martínez R., and Moy, C.M., 2010, Covariability of the Southern Westerlies and atmospheric CO2 during the Holocene. Geology, v. 38, p. 727-730.

Nishiizumi, K., Imamura, M., Caffee, M.W., Southon, J.R., Finkel, R.C., McAninch, J., 2007, Absolute calibration of Be-10 AMS standards: Nuclear Instrum. Methods Phys. Res. Sect. B, v. 258, p. 403–413.

Oerlemans, J., 2005, Extracting a Climate Signal from 169 Glacier Records: Science v. 308, p. 675-677.

Pigati, J.S. and Lifton, N.A., 2004, Geomagnetic effects on time-integrated cosmogenic nuclide production with emphasis on in situ $_{14}$C and $_{10}$Be: Earth and Planet. Sci. Lett., v. 226, p. 193-205.

Putnam, A.E., Denton, G.H., Schaefer, J.M., Barrell, D.J.A., Andersen, B.G., Finkel, R.C., Schwartz, R., Doughty, A.M. Kaplan, M.R., Schlüchter. C., 2010a, Glacier

advance in southern middle-latitudes during the Antarctic Cold Reversal: Nature Geoscience, v. 3, p. 700-704.
Putnam, A.E., Schaefer, J.M., Vandergoes, M., Barrell, D., Kaplan, M., Goehring, B., Schwartz, R., Finkel, R., Kelley, S., Denton, G.H., 2010b, In situ cosmogenic 10Be production-rate calibration from the Southern Alps, New Zealand: Quaternary Geochronology, v. 5, p. 392–409.
Reimer, P.J. and 26 more, 2009, IntCal09 and Marine09 radiocarbon age calibration curves, 0–50,000 years cal BP: Radiocarbon, v. 51, p. 1111-1150.
Rignot, E., Rivera, A., Casassa, G., 2003, Contribution of the Patagonia Icefields of South America to Sea Level Rise: Science v. 302, p. 434-436.
Schaefer J.M., Denton, G.H., Kaplan, M., Putnam, A., Finkel, R.C., Barrell, D.J.A., Andersen, B.G., Schwartz, R., Mackintosh, A., Chinn, T., Schlüchter, C., 2009, High-Frequency Holocene Glacier Fluctuations in New Zealand Differ from the Northern Signature: Science, v. 324, p. 622-625 (SOM).
Stone, J.O., 2000, Air pressure and cosmogenic isotope production: J. Geophys. Res., v. 105, p. 23753- 23759.
Strelin J.A., Denton, G.H., Vandergoes, M.J., Ninnemann, U.S., Putnam, 2011, A.E. Radiocarbon chronologies of the lateglacial Puerto Bandera Moraines, southern Patagonian Icefield, Argentina: Quaternary Science Reviews 30, p. 2551-2569.
Turney, C.S.M., Roberts, R.G., de Jonge, N., Prior, C., Wilmshurst, J.M., McGlone, M.S., Cooper, J., 2007, Redating the advance of the New Zealand Franz Josef Glacier during the Last Termination: evidence for asynchronous climate change: Quaternary Science Reviews, v. 26, p. 3037-3042.
Warren. C.R and Sudgen, D.E., 1993, The Patagonian Icefields: A Glaciological Review: Arctic and Alpine Research, v. 25, p., 316-331.

FIGURE CAPTIONS

Figure DR1. Satellite image showing physiographical attributes of the Laguna Azul-Lago Sarmiento Area and surrounding terrain. From the Vega Baguales meltwater channel, a calibrated age of 12,500 ± 70 cal yr B.P. (this study) is a minimum-limiting age for deglaciation from TDP II, III, and IV moraines and closely agrees with the deglacial ages published by Moreno et al. (2009). A deglacial age of 12,500 cal yr B.P. agrees with the ACR age for the TDPII, III, and IV moraines.

Figure DR2. Examples of boulders sampled for ^{10}Be exposure dating from TDP II, III, and IV moraines at Torres del Paine. Photographs show moraines and boulders at different parts of the study area. See Fig. 3 in main manuscript for location and ages, and Table DR1 for samples details.

Figure DR3. Distribution of the analytical errors in the Torres del Paine moraine dataset (n=30; two recalculated samples from Moreno et al., (2009). More than 90 percent of the individual analytical errors are <5% and two samples (6-7 percent) yielded errors 6-8%.

Figure DR4. Vega Baguales (50º53’47’’S; 72º44’35’’W, 455 m a.s.l.) stratigraphic column. A ^{14}C sample was obtained from a gastropod layer at 272 cm and yielded a

calibrated age of 12,500 ± 70 yr B.P. (radiocarbon age of 10,550 ± 55 years B.P.). See text for details.

Figure DR5. Probability plots without outliers for each TDP moraine belt. The thin curves represent individual sample ages ± 1σ. The thick curve is the summed normalized probability distribution of the moraine age population. Central vertical lines in plots denote the arithmetic mean ±1σ (yellow rectangle), 2σ (red vertical line) and 3σ (green vertical line). Values used in the text are arithmetic means and associated uncertainties obtained after rejecting outliers. Uncertainties used (bolded values) include propagation of the analytical and production-rate errors. We used a 2.4% uncertainty from the ^{10}Be production rate as defined in Putnam et al. (2010b). a – TDP II moraine; b – TDP III moraine; c – TDPIV moraine.

a. TDP II moraine belt, no outliers. Samples (n= 14):
LA0703, 07, 15, 20, 0901
RP0815, 17, 20
SAR0703, 05, 13, 18, 25, 0907

<u>Statistics</u>
Arithmetic mean/1 sigma uncertainty: 14,200±420 yrs
Including production rate uncertainty: **14,200±540 yrs**
Weighted mean/weighted uncertainty: 14,200±100 yrs
Peak age: 14,200 yrs
Median/Interquartile Range: 14,100±580 yrs
Reduced χ^2: 0.9

b. TDP III moraine belt, no outliers. Samples (n=10):
LA0522, 0704, 27, 28
RP0705, 0903, 04, 05, 06
SAR0908

<u>Statistics</u>
Arithmetic mean/1 sigma uncertainty: 14,100±420 yrs
Including production rate uncertainty: **14,100±540 yrs**
Weighted mean/weighted uncertainty: 14,100±150 yrs
Peak age: 14,000 yrs
Median/Interquartile Range: 14,000±590 yrs
Reduced χ^2: 0.4

c. TDP IV moraine belt, no outliers and recalculated ages (samples VN-05-25, 26) from Moreno et al. (2009). Samples (n=6):
RP0701, 03
SAR0721, 23
VN0525, 26

Statistics
Arithmetic mean/1 sigma uncertainty: 14,100±600 yrs
Including production rate uncertainty: **14,100±690 yrs**
Weighted mean/weighted uncertainty: 14,000±190 yrs
Peak age: 13,900 yrs
Median/Interquartile Range: 13,900±360 yrs
Reduced χ^2: 1.1

Table DR1. Geographical and ^{10}Be Analytical Data for TDP II, III, IV Moraines Cosmogenic Samples.

SAMPLE ID	Lat ºS	Long ºW	Elevation (m a.s.l.)	Sample thickness (cm)	Boulder height (cm)	Shielding correction	^{10}Be ±1σ (10^4 atoms g^{-1})	^{10}Be/^{9}Be ratio ± error	^{10}Be Standarization
TDPII moraine ridges									
LA0714	-50,9064	-72,7486	442	1,8	361,0	0,990	5.76±0.42	1.47E-14 ± 1.08E-15	07KNSTD
LA0715	-50,9067	-72,7483	435	1,1	238,0	0,990	8.67±0.31	3.98E-14 ± 1.40E-15	07KNSTD
LA0716	-50,9106	-72,7478	379	0,7	338,0	0,990	10.00±0.34	3.98E-14 ± 1.36E-15	07KNSTD
LA0720	-50,9119	-72,7481	376	2,6	155,0	0,990	8.06±0.36	2.82E-14 ± 1.24E-15	07KNSTD
SAR0718	-50,9869	-72,6919	146	3,2	176,0	0,990	6.54±0.24	3.47E-14 ± 1.29E-15	07KNSTD
LA0732	-50,9303	-72,7283	266	1,7	245,0	1,000	11.41±0.42	2.96E-14 ± 1.10E-15	07KNSTD
SAR0719	-50,9764	-72,6550	146	1,2	114,0	0,990	6.00±0.31	1.65E-14 ± 8.61E-16	07KNSTD
SAR0702	-50,9903	-72,7070	261	1,1	135,0	0,999	6.97±0.20	2.70E-14 ± 7.93E-16	07KNSTD
SAR0703	-50,9900	-72,7062	257	1,4	253,0	0,999	7.61±0.21	3.73E-14 ± 1.01E-15	07KNSTD
SAR0705	-50,9781	-72,6861	188	1,4	284,0	1,000	6.84±0.19	3.73E-14 ± 1.02E-15	07KNSTD
SAR0713	-50,9861	-72,7342	296	1,0	188,0	1,000	7.93±0.20	4.01E-14 ± 1.01E-15	07KNSTD
SAR0725	-50,9919	-72,7322	312	1,9	163,0	1,000	7.79±0.21	3.75E-14 ± 1.02E-15	07KNSTD
SAR0907	-50,9948	-72,7123	299	0,9	70,0	0,999	7.92±0.16	5.47E-14 ± 1.10E-15	07KNSTD
LA0703	-50,8867	-72,7378	386	1,1	178,0	0,996	8.71±0.25	2.90E-14 ± 8.19E-16	07KNSTD
LA0707	-50,8892	-72,7286	353	1,9	284,0	0,999	8.40±0.18	4.47E-14 ± 9.74E-16	07KNSTD
LA0901	-50,8891	-72,7272	350	1,8	89,0	1,000	8.07±0.17	4.18E-14 ± 8.82E-16	07KNSTD
RP0815	-50,9344	-72,7281	227	2,5	145,0	1,000	7.48±0.23	3.90E-14 ± 1.22E-15	07KNSTD
RP0817	-50,9483	-72,7321	286	1,2	203,0	0,999	8.22±0.28	4.26E-14 ± 1.46E-15	07KNSTD
RP0820	-50,9520	-72,7360	304	1,4	190,0	1,000	7.45±0.28	2.70E-14 ± 1.03E-15	07KNSTD

Table DR1. Geographical and ^{10}Be Analytical Data for TDP II, III, IV Moraines Cosmogenic Samples (continued).

SAMPLE ID	Lat ºS	Long ºW	Elevation (m a.s.l.)	Sample thickness (cm)	Boulder height (cm)	Shielding correction	^{10}Be ±1σ (10^4 atoms g^{-1})	^{10}Be/^{9}Be ratio ± error	^{10}Be Standarization
TDPIII moraine ridges									
LA0727	-50,9058	-72,7644	350	0,7	146,0	0,990	8.44±0.32	3.53E-14 ± 1.32E-15	07KNSTD
LA0728	-50,9033	-72,7592	364	1,0	279,0	0,990	8.04±0.30	4.08E-14 ± 1.53E-15	07KNSTD
LA0512	-50,8896	-72,7563	465	2,5	147,0	0,998	7.15±0.34	2.26E-14 ± 1.06E-15	07KNSTD
LA0522	-50,8968	-72,7620	423	2,0	83,0	0,990	9.19±0.77	1.52E-14 ± 1.27E-15	07KNSTD
SAR0724	-51,0011	-72,7481	311	0,9	149,0	0,990	10.41±0.54	2.58E-14 ± 1.34E-15	07KNSTD
LA0704	-50,8867	-72,7378	358	0,8	199,0	0,998	8.10±0.21	4.21E-14 ± 1.07E-15	07KNSTD
SAR0701	-50,9906	-72,6971	192	1,3	89,0	0,999	4.38±0.16	3.04E-14 ± 1.12E-15	07KNSTD
SAR0906	-50,9929	-72,7016	207	1,6	106,0	1,000	3.77±0.24	1.52E-14 ± 9.51E-16	07KNSTD
SAR0908	-50,9975	-72,7273	307	1,4	99,0	1,000	7.83±0.32	4.81E-14 ± 1.99E-15	07KNSTD
RP0903	-50,9436	-72,7516	234	0,7	157,0	1,000	7.30±0.19	6.28E-14 ± 1.62E-15	07KNSTD
RP0904	-50,9469	-72,7566	245	1,1	94,0	1,000	7.38±0.32	2.30E-14 ± 9.98E-16	07KNSTD
RP0905	-50,9482	-72,7575	245	1,2	83,0	1,000	7.23±0.34	3.09E-14 ± 1.45E-15	07KNSTD
RP0906	-50,9536	-72,7633	266	0,9	84,0	1,000	7.58±0.20	6.38E-14 ± 1.68E-15	07KNSTD
RP0705	-50,9203	-72,7853	441	1,3	161,0	1,000	9.10±0.26	5.94E-14 ± 1.72E-15	07KNSTD

Table DR1. Geographical and ^{10}Be Analytical Data for TDP II, III, IV Moraines Cosmogenic Samples (continued).

SAMPLE ID	Lat ºS	Long ºW	Elevation (m a.s.l.)	Sample thickness (cm)	Boulder height (cm)	Shielding correction	^{10}Be ±1σ (10^4 atoms g^{-1})	^{10}Be/^{9}Be ratio ± error	^{10}Be Standarization
TDPIV moraine ridges									
SAR0721	-51,0019	-72,7311	242	1,0	142,0	1,000	8.08±0.33	4.99E-14 ± 2.01E-15	07KNSTD
RP0701	-50,9097	-72,7998	375	1,2	165,0	0,999	8.19±0.21	6.78E-14 ± 1.78E-15	07KNSTD
RP0703	-50,9225	-72,7878	404	1,2	180,0	1,000	8.46±0.28	3.61E-14 ± 1.20E-15	07KNSTD
SAR0722	-51,0036	-72,7353	251	2,6	249,0	0,990	8.55±0.49	1.93E-14 ± 1.10E-15	07KNSTD
SAR0723	-51,0022	-72,7547	318	2,3	158,0	0,990	7.64±0.49	1.18E-14 ± 7.54E-16	07KNSTD
VN-05-25	-50,9470	-72,7863	218	0,9	135,0	1,000	8.06±0.26	7.37E-14 ± 2.46E-15	07KNSTD
VN-05-26	-50,9489	-72,7879	204	2,8	92,0	1,000	7.71±0.22	7.18E-14 ± 2.04E-15	07KNSTD

All samples measured at CAMS using the 2.85×10^{-12} = 07KNSTD3110 standard for normalization (Nishiizumi et al., 2007). 07knstd ^{10}Be/^{9}Be = $(2.79 \pm 0.03) \times 10^{-11}$.

We added to all samples, including five procedural blanks (^{10}Be/^{9}Be= $2*10^{-16}$), 0.2 mg of the ^{9}Be carrier (concentration = 996 ppm), except for samples LA0522, LA0714, LA0732, SAR0719, SAR0722, SAR0723, SAR0724, which were spiked with 0.18 mg of the ^{9}Be carrier.

VN samples= Published by Moreno et al. (2009) and recalculated here.

Table DR2. ^{10}Be Ages for Torres del Paine TDP II, III and IV Moraines Cosmogenic Samples.

SAMPLE ID	Lm int ext	Du int ext	Li int ext	De int ext	Cronus PR** Lm int ext
TDPII moraine ridges					
LA0714*	**9300 ± 680 710**	9500 ± 700 730	9300 ± 690 710	9400 ± 690 720	7900 ± 570 890
LA0715	**13900 ± 490 580**	14300 ± 510 590	14100 ± 500 570	14100 ± 500 580	11900 ± 410 1090
LA0716*	**16900 ± 580 690**	17300 ± 600 700	17000 ± 590 670	17100 ± 590 690	14400 ± 490 1320
LA0720	**13800 ± 610 680**	14200 ± 630 700	14000 ± 620 670	14000 ± 620 680	11900 ± 510 1130
SAR0718	**13900 ± 520 600**	14300 ± 530 610	14000 ± 520 590	14000 ± 520 600	12000 ± 430 1110
LA0732*	**21300 ± 800 920**	21800 ± 820 940	21400 ± 800 900	21500 ± 800 920	18300 ± 670 1690
SAR0719*	**12600 ± 660 720**	12900 ± 680 730	12700 ± 670 710	12700 ± 670 720	10800 ± 550 1080
SAR0702*	**13000 ± 380 480**	13400 ± 400 480	13100 ± 390 460	13100 ± 390 470	11100 ± 320 1000
SAR0703	**14300 ± 390 500**	14700 ± 400 500	14400 ± 390 480	14400 ± 390 490	12200 ± 330 1090
SAR0705	**13700 ± 380 480**	14000 ± 380 480	13800 ± 380 460	13800 ± 380 470	11700 ± 310 1040
SAR0713	**14300 ± 360 470**	14700 ± 370 480	14400 ± 360 460	14500 ± 370 470	12300 ± 300 1080
SAR0725	**13900 ± 380 480**	14300 ± 390 490	14100 ± 380 470	14100 ± 380 480	12000 ± 320 1060
SAR0907	**14300 ± 290 420**	14700 ± 300 430	14400 ± 290 400	14400 ± 290 420	12200 ± 240 1060
LA0703	**14600 ± 410 520**	15000 ± 420 530	14700 ± 420 500	14700 ± 420 520	12500 ± 340 1110
LA0707	**14500 ± 320 450**	14900 ± 330 450	14600 ± 320 430	14700 ± 320 440	12400 ± 270 1090
LA0901	**14000 ± 300 420**	14400 ± 300 430	14100 ± 300 400	14100 ± 300 420	12000 ± 250 1040
RP0815	**14600 ± 460 560**	14900 ± 470 570	14700 ± 460 540	14700 ± 460 550	12500 ± 380 1130
RP0817	**15000 ± 520 610**	15400 ± 530 620	15100 ± 520 600	15200 ± 520 610	12900 ± 430 1170
RP0820	**13400 ± 510 590**	13800 ± 530 600	13500 ± 520 580	13600 ± 520 590	11500 ± 430 1060

Table DR2. ^{10}Be Ages for Torres del Paine TDP II, III and IV Moraines Cosmogenic Samples (continued).

SAMPLE ID	Lm int ext	Du int ext	Li int ext	De int ext	Cronus PR** Lm int ext
TDPIII moraine ridges					
LA0727	**14600 ± 550 630**	15000 ± 570 650	14800 ± 560 620	14800 ± 560 640	12500 ± 460 1160
LA0728	**13800 ± 520 600**	14200 ± 530 610	13900 ± 520 590	13900 ± 530 600	11800 ± 430 1090
LA0512*	**11200 ± 530 580**	11600 ± 550 600	11300 ± 540 580	11400 ± 540 590	9600 ± 440 930
LA0522	**15000 ± 1260 1300**	15500 ± 1290 1330	15200 ± 1270 1300	15200 ± 1270 1310	12900 ± 1050 1530
SAR0724*	**18700 ± 980 1060**	19200 ± 1000 1080	18800 ± 980 1050	18900 ± 990 1060	16000 ± 820 1590
LA0704	**13800 ± 350 460**	14200 ± 360 470	14000 ± 360 450	14000 ± 360 460	11900 ± 290 1050
SAR0701*	**8700 ± 320 370**	9000 ± 330 380	8800 ± 320 370	8800 ± 330 370	7500 ± 270 690
SAR0906*	**7400 ± 470 490**	7700 ± 480 500	7500 ± 470 490	7500 ± 470 500	6400 ± 390 670
SAR0908	**14000 ± 580 660**	14400 ± 600 670	14100 ± 590 650	14200 ± 590 660	12000 ± 490 1130
RP0903	**13900 ± 360 470**	14300 ± 370 480	14100 ± 370 460	14100 ± 370 470	11900 ± 300 1060
RP0904	**14000 ± 610 680**	14400 ± 630 690	14100 ± 610 670	14100 ± 620 680	12000 ± 510 1140
RP0905	**13700 ± 650 710**	14100 ± 670 730	13800 ± 650 710	13800 ± 650 710	11700 ± 540 1140
RP0906	**14100 ± 370 480**	14500 ± 380 490	14200 ± 370 460	14200 ± 370 480	12000 ± 310 1070
RP0705	**14400 ± 420 520**	14800 ± 430 530	14600 ± 420 510	14600 ± 420 520	12400 ± 350 1110

Table DR2. ^{10}Be Ages for Torres del Paine TDP II, III and IV Moraines Cosmogenic Samples (continued).

SAMPLE ID	Lm int ext†	Du int ext	Li int ext	De int ext	Cronus PR** Lm int ext
TDPIV moraine ridges					
SAR0721	**15300 ± 620 700**	15700 ± 640 720	15500 ± 630 690	15500 ± 630 700	13100 ± 520 1230
RP0701	**13800 ± 360 470**	14200 ± 370 480	13900 ± 370 460	14000 ± 370 470	11800 ± 300 1050
RP0703	**13900 ± 460 550**	14300 ± 470 560	14000 ± 470 540	14000 ± 470 550	11900 ± 390 1080
SAR0722*	**16400 ± 940 1000**	16800 ± 940 1020	16500 ± 940 1000	16600 ± 950 1010	14100 ± 790 1440
SAR0723	**13800 ± 890 940**	14100 ± 910 960	13900 ± 900 930	13900 ± 900 940	11800 ± 740 1260
VN-05-25	**14100 ± 450 550**	14500 ± 470 560	14300 ± 460 540	14300 ± 460 550	12100 ± 380 1100
VN-05-26	**13900 ± 400 500**	14200 ± 410 510	14000 ± 400 490	14000 ± 400 500	11900 ± 340 1070

† ^{10}Be ages: arithmetic mean ± internal (AMS) and external error (production rate).

* Outliers

** CRONUS ^{10}Be production rate as calculated in Balco et al. (2008).

Note: ^{10}Be ages in years calculated with four different scaling protocols (Balco et al., 2008). 'Lm' is the time dependent version of Stone/Lal scaling scheme (Stone, 2000). 'Du' is calculated using the scaling scheme of Dunai (2001), 'Li' the scaling based on Pigati anf Lifton (2004) and Lifton et al., (2008), and the 'De' scaling scheme presented in Desilets and Zreda (2003). All ages were calculated using a ^{10}Be production rate measured at New Zealand's Macaulay site (Putnam et al., 2010b), recently confirmed for the nearby Lago Argentino area in southern Patagonia (Fig. 1; Kaplan et al., 2011) except for last column with asterisk, which is calculated with the "CRONUS calibration data set" (Balco et al., 2008). We use the Lm scaling scheme (Stone, 2000) in our result discussion. Density of rock used for calculating ^{10}Be ages is 2.65 g cm^{-3}. Age uncertainties include internal (int) analytical error only and external error (ext), which includes systematic uncertainties (Balco et al., 2008) associated with scaling to the latitude and altitude of Torres del Paine region. VN samples= published by Moreno et al. (2009) and recalculated here.

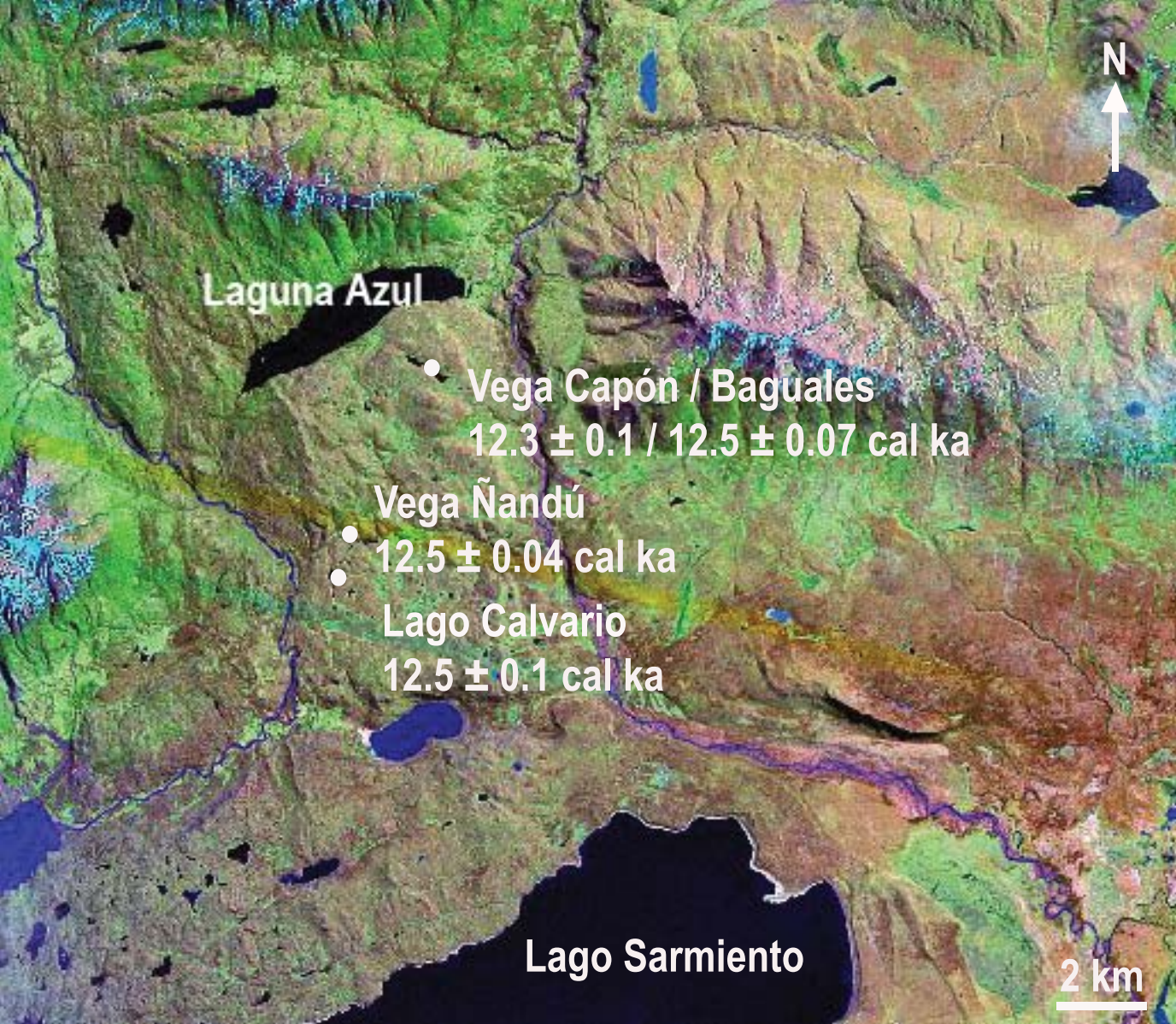
N
Laguna Azul
Vega Capón / Baguales
12.3 ± 0.1 / 12.5 ± 0.07 cal ka
Vega Ñandú
12.5 ± 0.04 cal ka
Lago Calvario
12.5 ± 0.1 cal ka
Lago Sarmiento
2 km

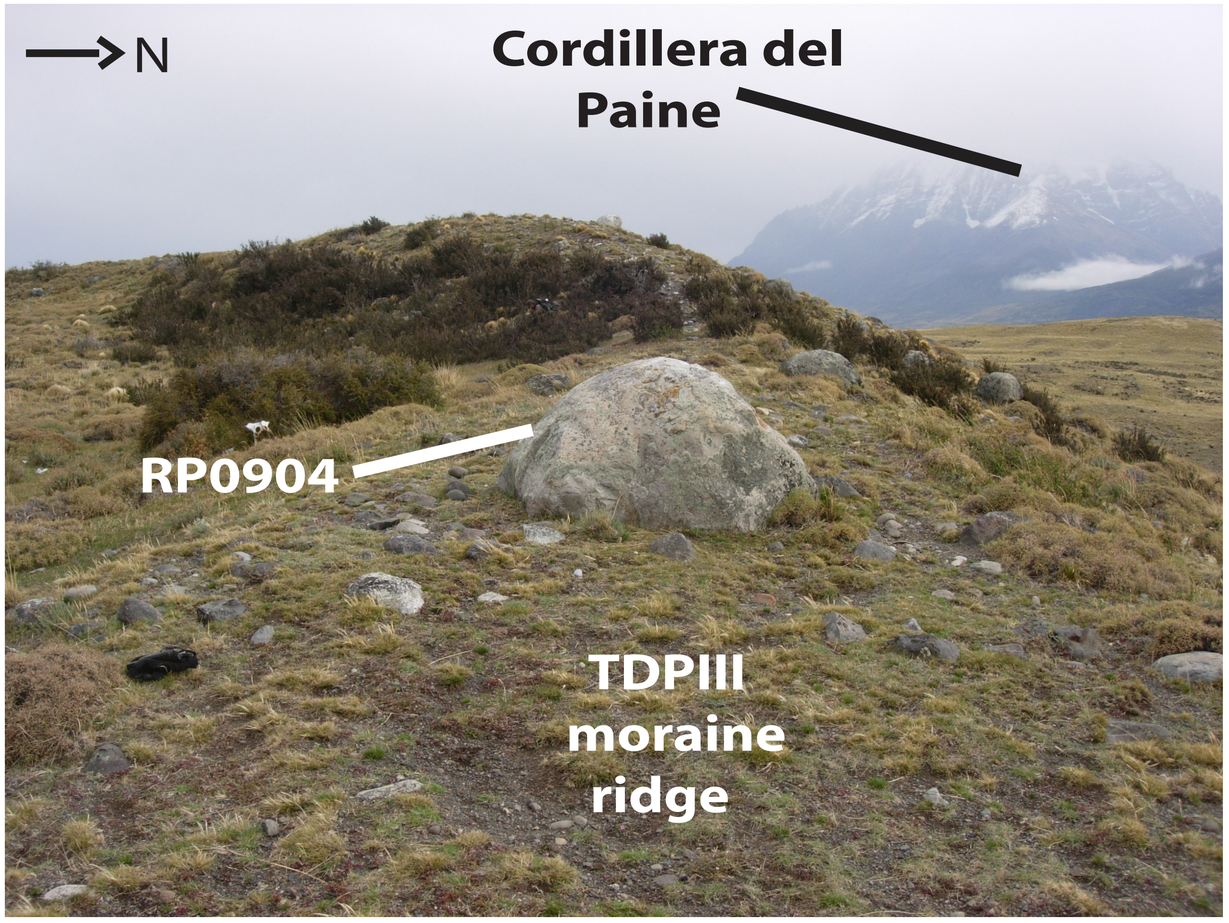
N
Cordillera del Paine
RP0904
TDPIII moraine ridge

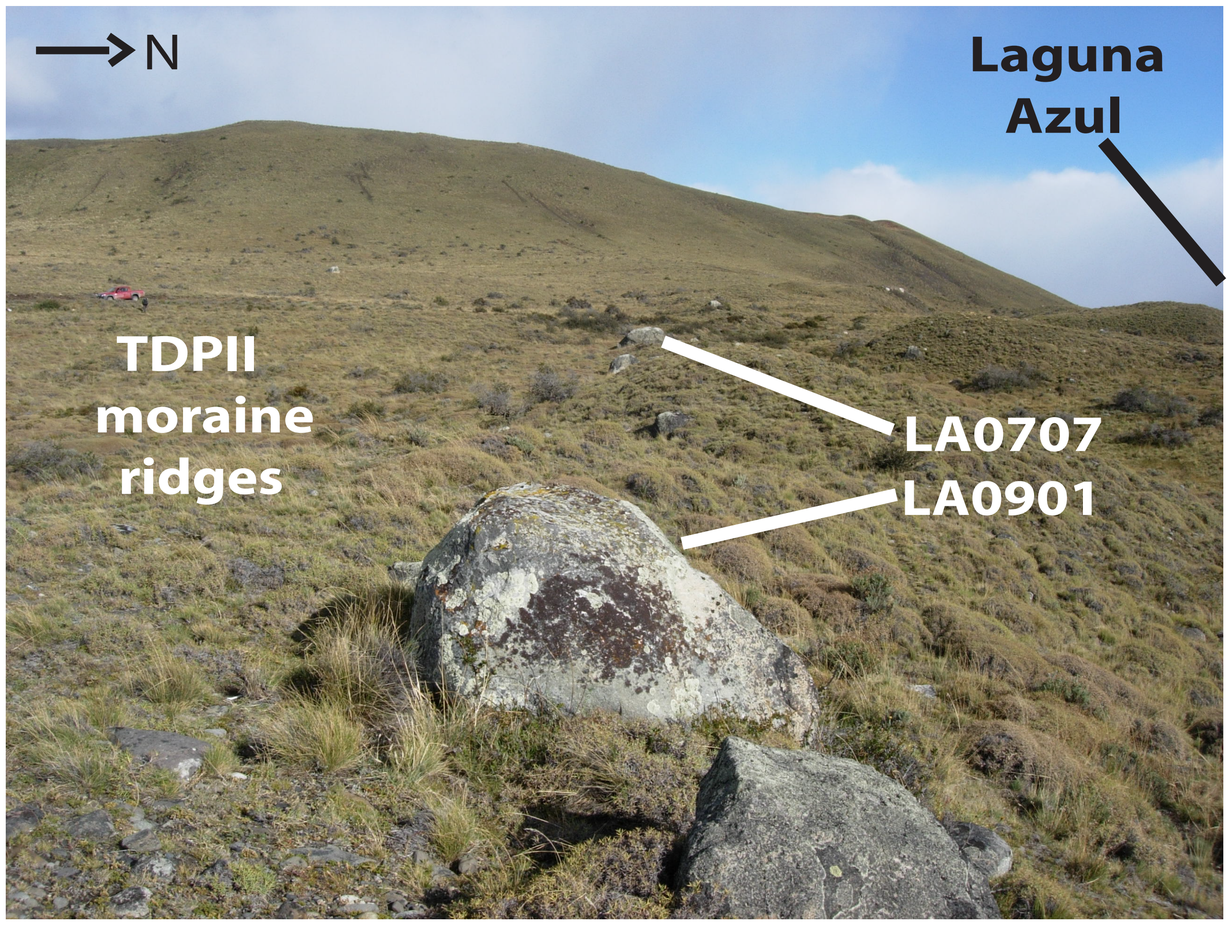
N
Laguna Azul
TDPII moraine ridges
LA0707
LA0901


N
SAR0908
TDPII moraine ridge

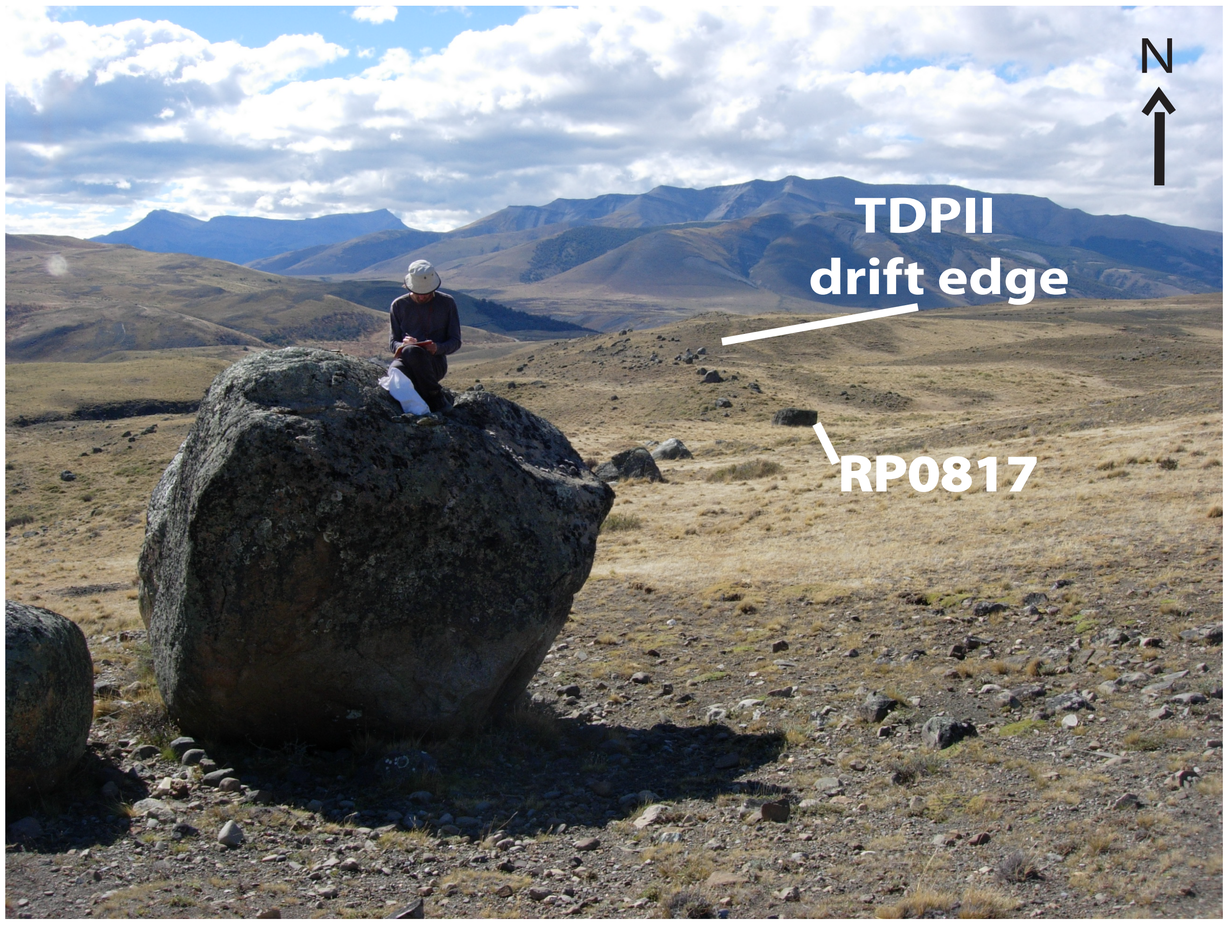
N
TDPII drift edge
RP0817

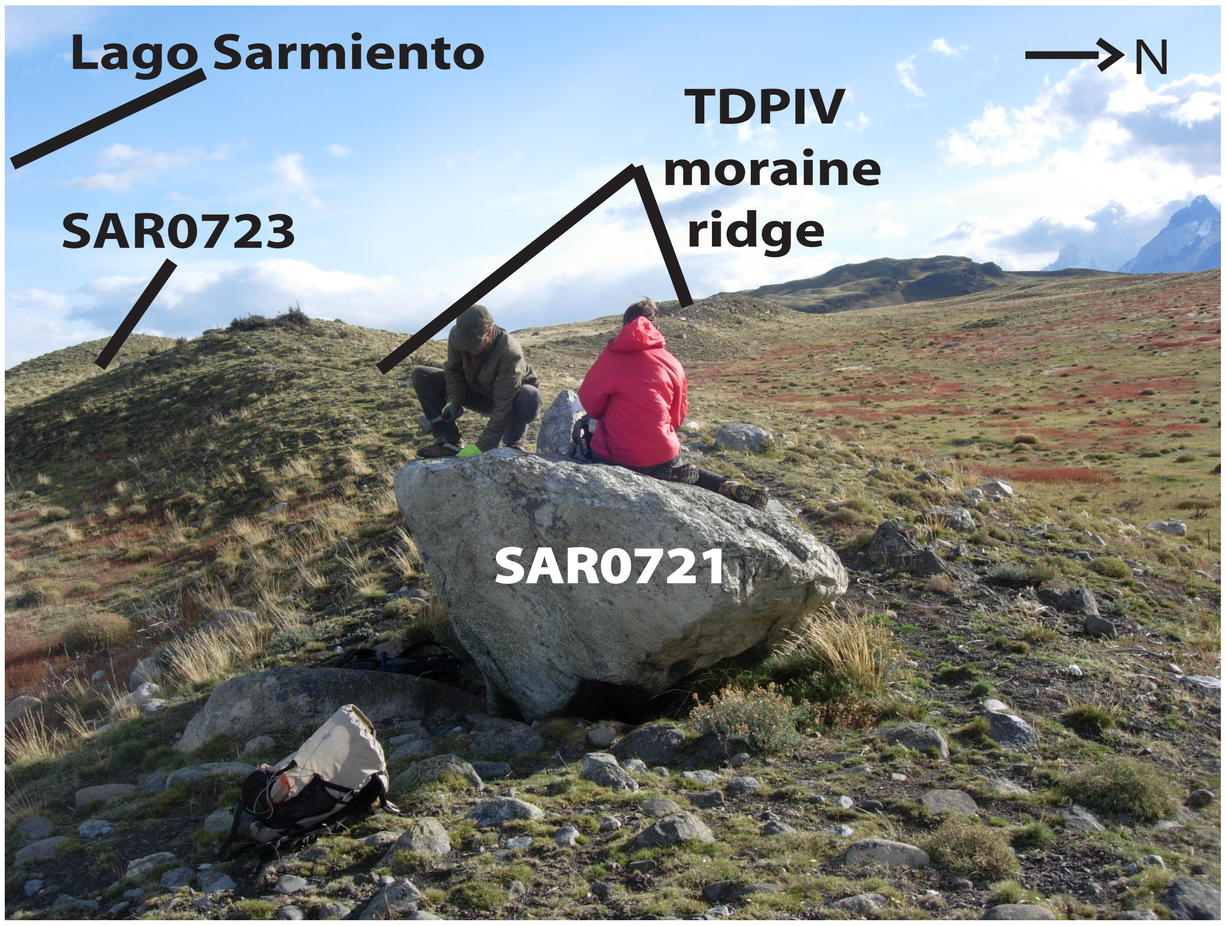
Lago Sarmiento
N
TDPIV moraine ridge
SAR0723
SAR0721

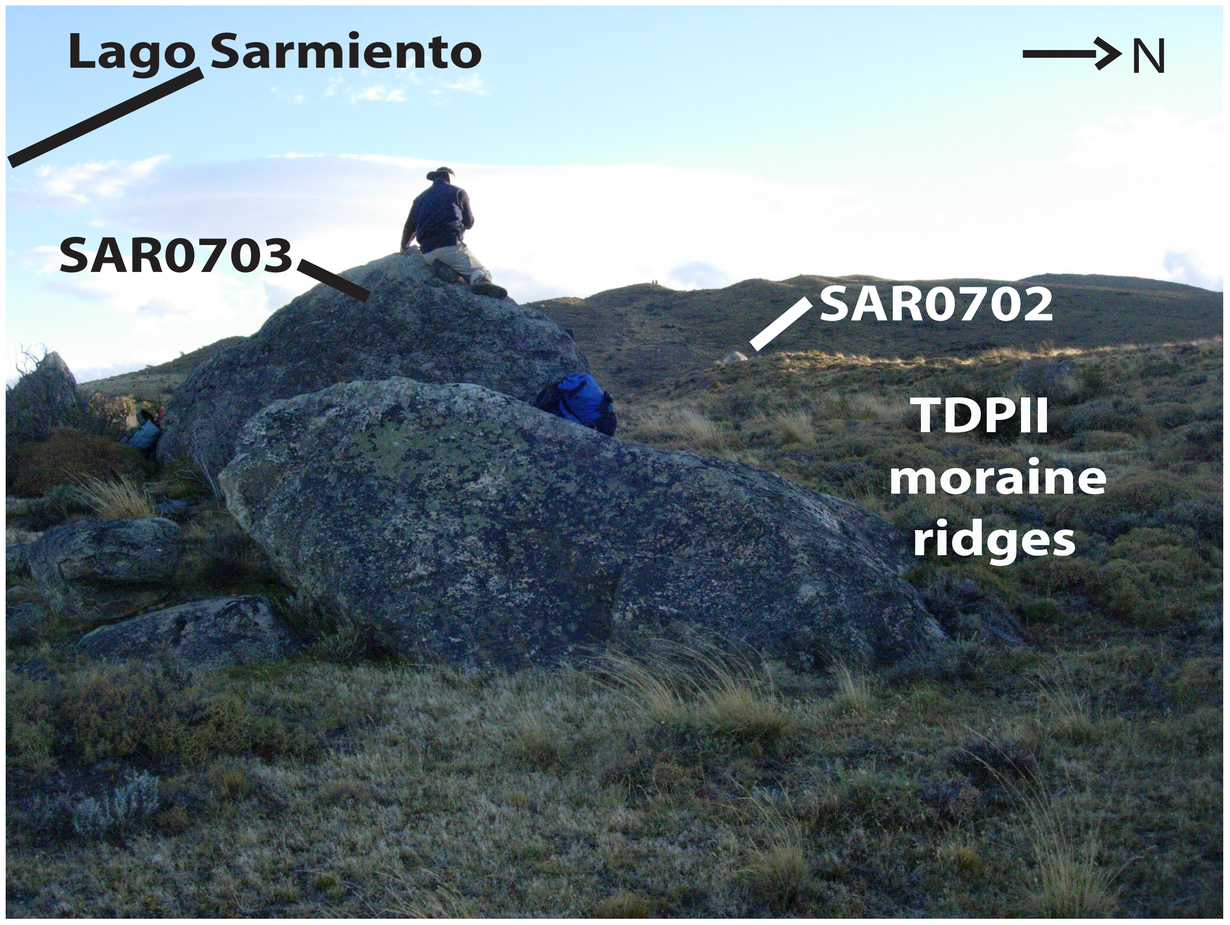
Lago Sarmiento
N
SAR0703
SAR0702
TDPII moraine ridges

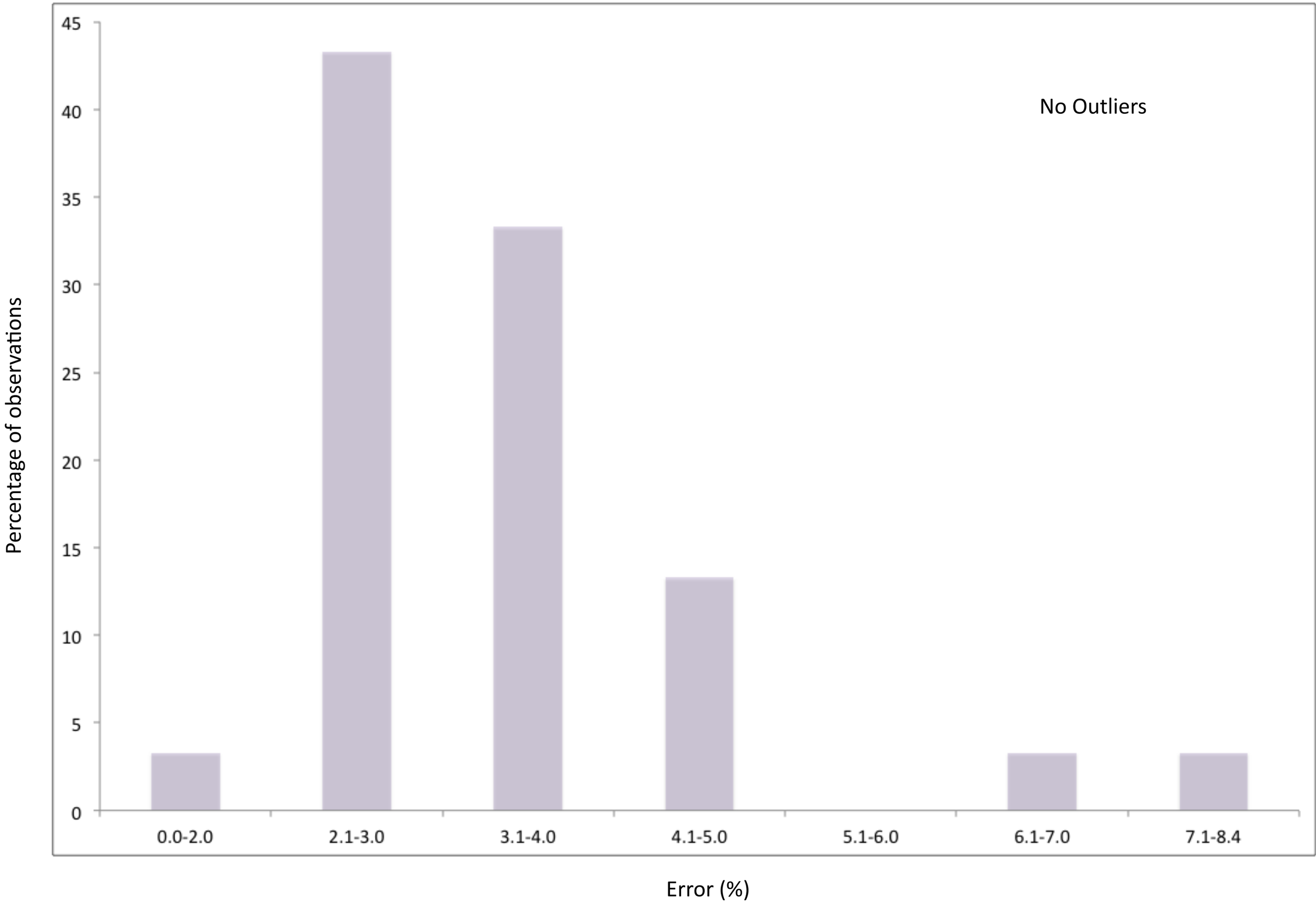
No Outliers
Percentage of observations
45
40
35
30
25
20
15
10
5
0
0.0-2.0
2.1-3.0
3.1-4.0
4.1-5.0
5.1-6.0
6.1-7.0
7.1-8.4
Error (%)

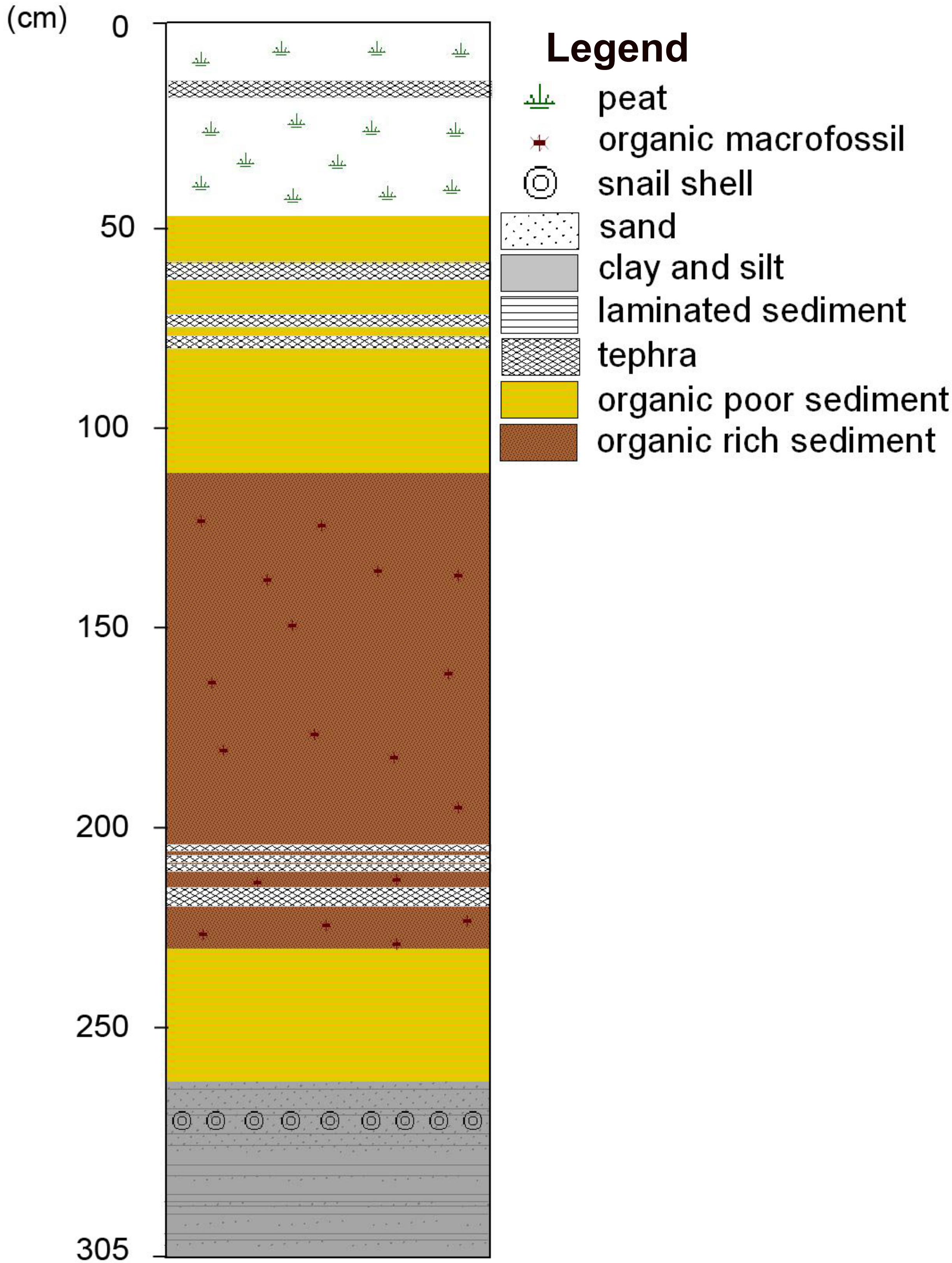
(cm)
0
50
100
150
200
250
305
Legend
peat
organic macrofossil
snail shell
sand
clay and silt
laminated sediment
tephra
organic poor sediment
organic rich sediment

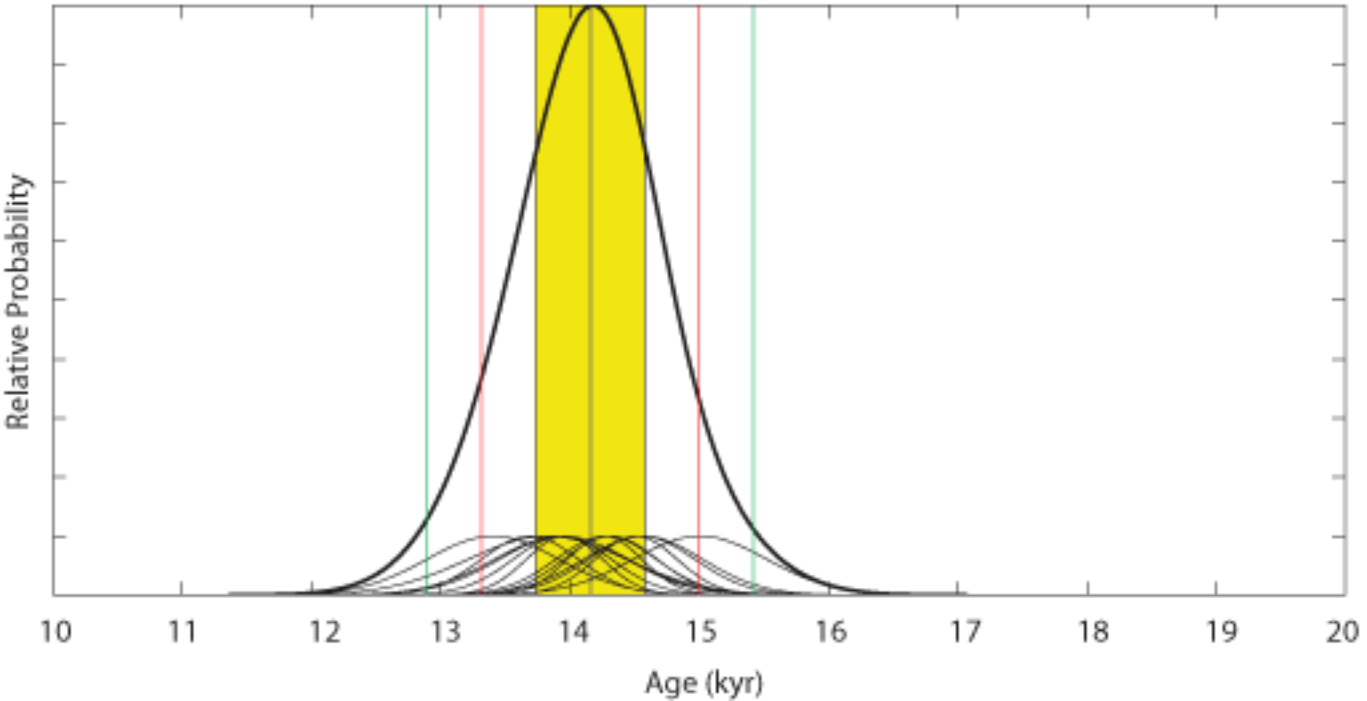
Relative Probability
10
11
12
13
14
15
16
17
18
19
20
Age (kyr)

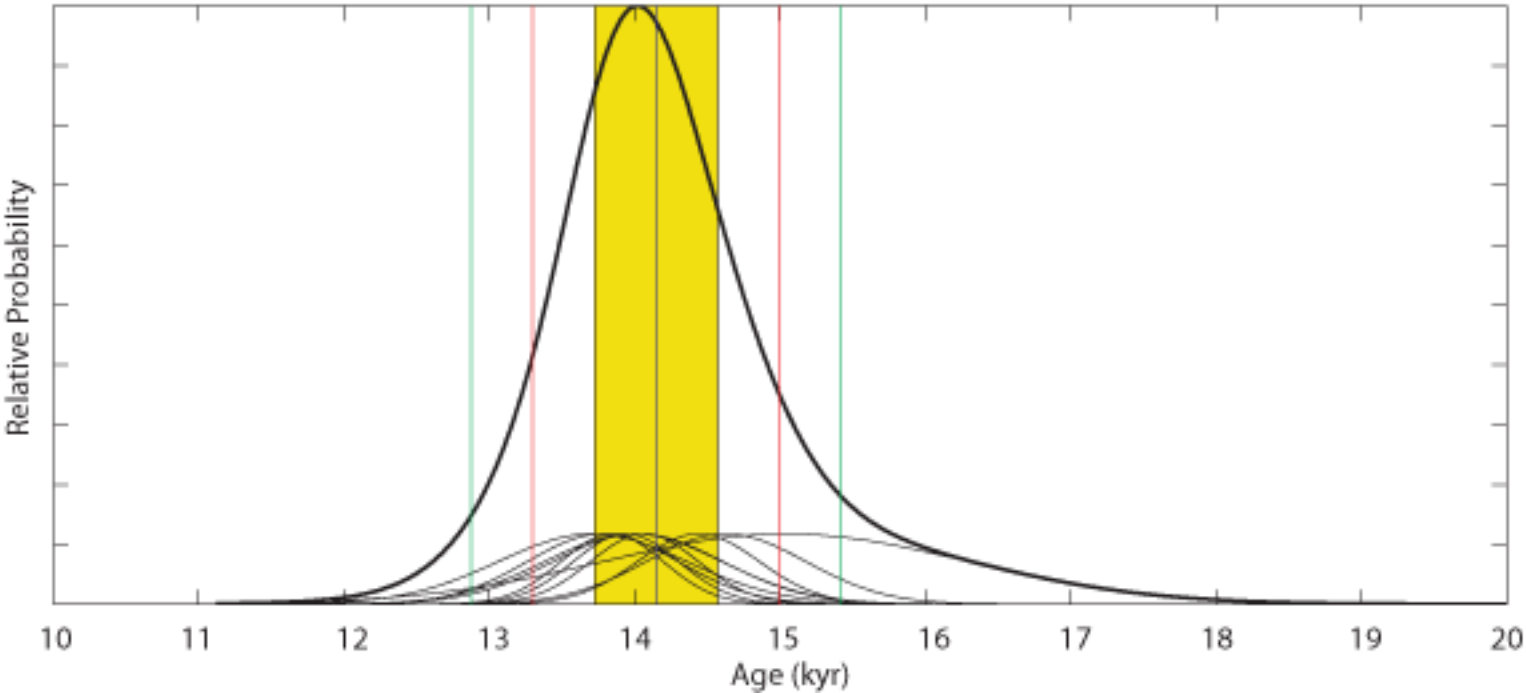
Relative Probability
10
11
12
13
14
15
16
17
18
19
20
Age (kyr)

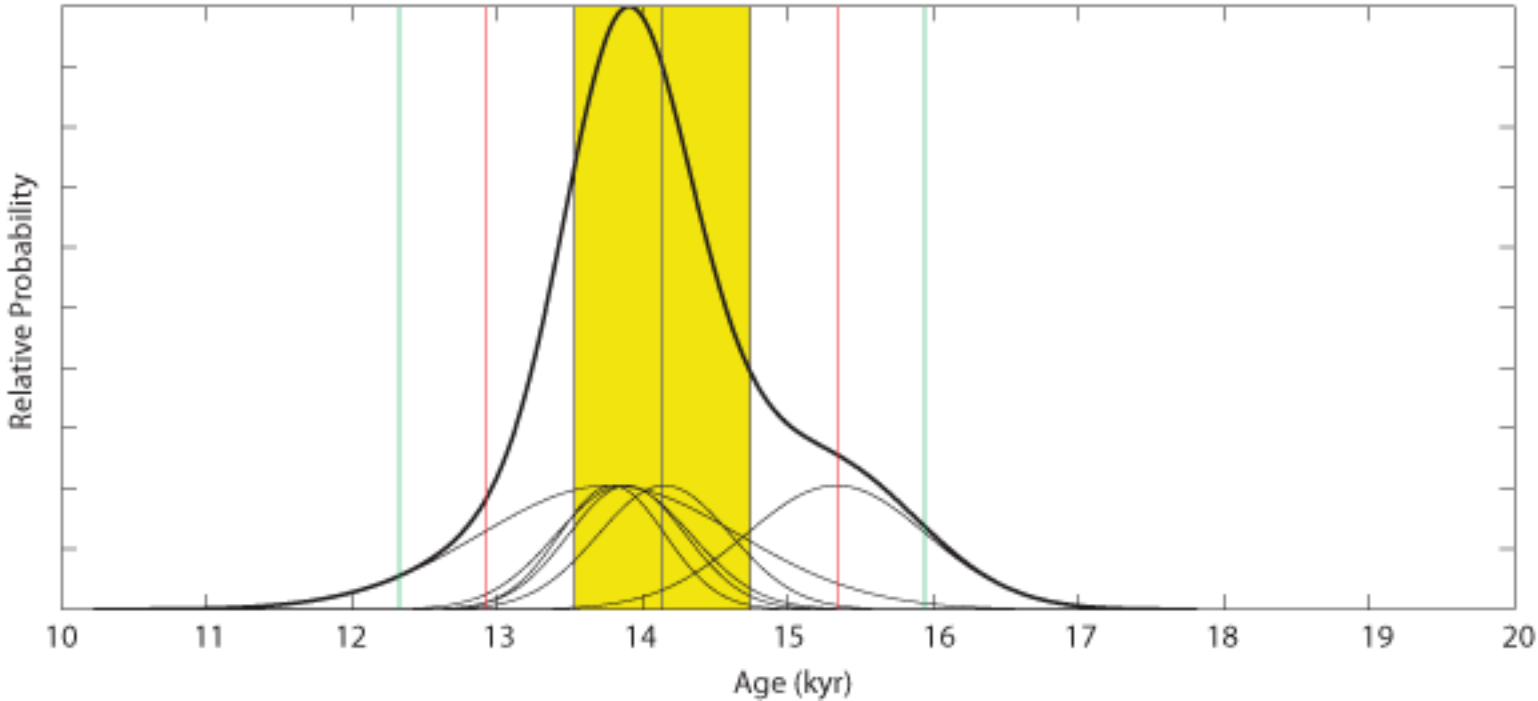
Relative Probability
10
11
12
13
14
15
16
17
18
19
20
Age (kyr)